First posted online on 11 June 2020 as 10.1242/jeb.215327
Access the most recent version at http://jeb.biologists.org/lookup/doi/10.1242/jeb.215327

How do hoverflies use their righting reflex?

Anna Verbe[1], Léandre P. Varennes[1], Jean-Louis Vercher[1] and Stéphane Viollet[1]*

[1]Aix Marseille Univ, CNRS, ISM, Marseille, France.

† Authors for correspondence: (stephane.viollet@univ-amu.fr)

ABSTRACT

When taking off from a sloping surface, flies have to reorient themselves dorsoventrally and stabilize their body by actively controlling their flapping wings. We have observed that the righting is achieved solely by performing a rolling manoeuvre. How flies manage to do this has not yet been elucidated. It was observed here for the first time that hoverflies' reorientation is entirely achieved within 6 wingbeats (48.8ms) at angular roll velocities of up to $10 \times 10^3 \ ^\circ/s$ and that the onset of their head rotation consistently follows that of their body rotation after a time-lag of 16ms. The insects' body roll was found to be triggered by the asymmetric wing stroke amplitude, as expected. The righting process starts immediately with the first wingbeat and seems unlikely to depend on visual feedback. A dynamic model for the fly's righting reflex is presented, which accounts for the head/body movements and the time-lag recorded in these experiments. This model consists of a closed-loop control of the body roll, combined with a feedforward control of the head/body angle. During the righting manoeuvre, a strong coupling seems to exist between the activation of the halteres (which measure the body's angular speed) and the gaze stabilization reflex. These findings again confirm the fundamental role played by the halteres in both body and head stabilisation processes.

KEYWORDS: Syrphidae, hoverflies, *Episyrphus balteatus*, **insect flight, body orientation, righting reflex**

Introduction

Righting reflex in animals has been investigated in a long series of experiments on vertebrates and invertebrates. Back in 1894, Etienne-Jules Marey was the first author to describe in detail how cats orient themselves as they fall (Marey (1894)). Hoverflies are known to use strategies based on bee, wasp or bumblebee body-colour mimicry, but they are completely defenceless as they cannot sting. These insects, which are among the main flying pollinators, are able to perform impressive aerobatic feats in complex environments (Wang (2005); Wystrach and Graham (2012); Mou et al. (2011)), such as hovering, in particular. Flies can land on all surfaces, including plants and walls, and they can even settle upside down on the ceiling (Liu et al. (2019)). Just after take-off, they have to adopt the normal right side up position in order to be able to fly: this particular action is called the righting reflex.

A classical approach to studying animals' righting reflex consists in dropping an animal into free fall with its legs pointing upwards. The animal will tend to rotate its body along its body axis and land on its legs. Some well-known experiments have been performed on these lines on mammalian taxa (Magnus (1924)) such as cats (Kane and Scher (1969)) and rats (Pellis et al. (1991)), and more recently on wingless insect species such as stick insects (Zeng et al. (2017)), ants (Yanoviak et al. (2010)) and aphids (Ribak et al. (2013); Meresman et al. (2014)). No free fall righting experiments of this kind have ever been performed so far to our knowledge, however, on flies with their legs pointing upwards.

Previous studies have shown that righting reflexes can involve two different mechanisms. Wingless animals use either an inertial or an aerodynamic control system to reorient themselves. During inertial righting processes, the falling animal orients segments of its body so as to create an instantaneous moment of inertia, which triggers a rotation of the body (Marsden and Ostrowski (1998)) by moving either the torso (as in cats and rodents), the legs (as in other mammalians, reptiles and amphibians) or the tail (as in lizards and kangaroo rats); whereas aerodynamic control occurs in wingless insects such as aphids, ants, and stick insects' larvae (see Jusufi et al. (2011)). When these animals perform appendicular movements (i.e., with their legs), bilaterally asymmetric forces induce a rotation of the body around its longitudinal axis (Jusufi et al. (2011); Ribak et al. (2013); Zeng et al. (2017)).

Fruit flies are able to produce torque from aerodynamic forces by generating asymmetric wing motion (Ristroph et al. (2010); Sane (2003); Beatus et al. (2015); Ristroph et al. (2013)). The present study focused on how the hoverfly controls its head and body-roll orientation, focusing in particular on the aerodynamic processes resulting in righting torque. Beatus et al. (Beatus et al. (2015)) have established that fruit flies can control their body-roll angle by establishing a stroke-amplitude asymmetry. Fruit flies can also generate active roll damping (60×10^3 °/s , see Beatus et al. (2015)) to stabilize their roll movements even when exposed to extreme speed perturbations within the duration of a single wingbeat, namely within 5ms. As fruit flies and blowflies are endowed with an efficient gaze stabilization reflex, which can be used to compensate for thorax rotations and thus to stabilize the visual world across the retina (Hardcastle and Krapp (2016); Taylor and Krapp (2007); Hengstenberg R. et al. (1986); Egelhaaf (2002)), head/body movements can be expected to occur during the righting process.

Based on previous studies on aerial righting reflexes (Zeng et al. (2017)), we developed a new experimental setup with which winged insects can be released from an upside-down position (see figure 1 and details in the Materials and Methods section). The present paper first describes the asymmetric wing movements triggering the body righting process, before addressing the kinematics of the hoverfly's righting reflex, focusing on the head, body and head/body angles. Results related to additional experiments (loaded halteres with glue, lighting from below, head-thorax glued) are presented and discussed. A dynamic model for the righting reflex involving both feedback and feedforward control systems is detailed. This model is consistent with a previously published control-block diagram of the fly's performances involving a proportional control of the roll movements based on the roll speed measured by the halteres (Beatus et al. (2015)). The halteres, which are two ancestral hindwings beating in anti-phase with the wings, are 'gyroscopic' sense organs which quickly measure the fly's rotational speed in space (Pringle and Gray (1948); Nalbach (1993); Hengstenberg (1998); Dickinson and Muijres (2016)). We also describe an additional feedforward mechanism possibly controlling the neck motor system, which accounts for the time-lag observed between the insects' head and body during the righting process. As suggested in previous studies and confirmed by an elegant recent model for the halteres' dynamics (Mohren et al. (2019)), the halteres act as body angular rate sensors which are sensitive to both Coriolis and centrifugal forces. In the present model, the halteres are involved in two nested feedback-loops controlling the roll rate and the roll angle and in the feedforward system, controlling the head orientation with respect to the thorax.

MATERIAL AND METHODS

Biological material

Episyrphus balteatus pupae were purchased from Katz Biotech AG, Baruth, Germany. They were fed with pollen and honey *ad libitum*. To facilitate the hoverflies' manipulation, a drop of iron glue (composed of 45% beeswax, 45% rosin and 10% iron dust) was placed on their thorax. Small cylindrical magnets (Supermagnete, Gottmadingen, Germany, diameter = 2mm, length = 1mm, weight = 23mg) magnetized with the iron glue were used to make manipulation of the insects with ceramic clamps easier and gentler. Flies were released upside-down from a suction based custom-built device. Its surface consisted of a downward-facing Teflon-coated plastic angled ridge, which minimized the occurrence of leg adhesion to the substrate. Suction was applied via a capillary glass tube (diameter approx. 1mm) introduced into a small hole in the middle of the plastic ridge. The device was attached to the top of the box, the horizontal position of which was monitored with a spirit level. The capillary tube was connected to a vacuum source, and the air pressure was valve-controlled. In each trial, the insect to be tested was placed on a Teflon-coated carrier surface, its mesosternum (i.e. the mid-thoracic ventral surface located near the center of mass) connected via suction to the opening of the capillary tube. Magnets were detached after transferring the insects to the device, before they were released. We always checked before each experiment whether the hoverflies equipped with the iron glue could fly in the breeding cages, in order to ensure that their flight abilities were not affected by the glue. A total number of 13 falls involving 4 males and 6 females were recorded.

Experimental set-up and protocols

Aerial righting performances were recorded with a high-speed video camera (Phantom Miro M11O) at a rate of 1600 frames per second (1280x800 pixels). The macro lens used (a Nikon Micro-Nikkor AF-S DX Micro 40mm f/2.8 G) gave a good compromise between size

of the fly, the resolution and the visual field (the fly-to-camera distance was about 20cm). Hoverflies were placed upside-down with a custom-built device inspired by Zeng et all (Zeng et al. (2017)). The insect tested was released by turning off the vacuum source. The experimental arena was covered with a white diffuser (PMMA WH02, 3mm thick) and illuminated from above by a halogen light (Kaiser Studiolight H; 5.6 x 10^{-13} $W.m^{2}$). An optic fibre ring light (Schott, KL 1500) connected to a halogen light source via an optic fiber (Xenophot HLX, OSRAM) was placed around the camera lens to enhance the quality and the brightness of the video. The camera was triggered automatically as soon as the insect entered the camera's field of view (Figure 1A).

Image processing and analysis.

As shown in figure 2, the wing positions were recorded from 2 pairs of natural markers (at the wing junction points and wing tips). In the head, body and head/body study, the positions of the hoverfly's body were indicated by 3 pairs of markers placed at the two pairs of legs (front and hind legs) and the wing junction points, and a single pair of markers placed at the top and bottom of the head was used to indicate the position of the head. All the trackers moving over a uniform background were recorded using the Tracker Video Analysis and Modeling Tool (Copyright (c) 2018 Douglas Brown, see figures 1B and D). The stroke amplitude of the left (ϕ_L) and right wings (ϕ_R) relative to the body's orientation were defined as the angle between the wing angle (wing junction and wing tip) and the body roll angle (at the junction between the two wings). The stroke plane angle could not be measured due to the orientation of the camera, but we were only interested here in the relative difference between the left and right wingbeat amplitudes. The head and body roll orientation relative to the vertical were estimated in this way during aerial righting (Figure 1C). To check the body roll orientation values (taking θ_{TR} to denote the Thorax Roll), we calculated the mean positions of the two pairs of legs and the orientation of the wing junction angle. The leg and wing vectors are orthogonal to the dorsoventral body orientation. To determine the head orientation (taking θ_{HR} to denote the Head Roll), the two head tracking points (top and bottom) were used (figure 1B and D). In the normal right-side up position (legs pointing downwards), head and body were taken to have a 0° inclination, while in the upside-down starting position (legs pointing upwards), head and body were taken to have an 180° inclination (figure 1A to B).

The θ_{HB} (Head/Body) angle consisted of the difference between the absolute head roll angle and the absolute thorax roll angle: $\theta_{HB} = \theta_{HR} - \theta_{TR}$. Cluster analyses of normalized wingbeat amplitude differences (see figure 2C) were performed with R (R Core Team (2019), www.R-project.org) while the rest of the analyses were performed with MATLAB (R2018a, MathWorks, Natick, MA, USA). The evolution with time of all the angles measured and the roll angle velocities (θ_{HB}) were calculated by applying a Savitzky–Golay filter (order 2, window: 35). As the body always rights before the complete reorientation of the head (see figure 3), it was assumed here that the righting reflex started with the first wingbeat and ended when θ_{HB} was equal to zero (i.e., when the head was realigned with the body). We therefore focused on the fly's body kinematics during this brief part of the fall.

Additional experiments confirming the validity of the model

In order to test the dynamic model for the righting reflex, we performed some supplementary experiments. In previous experiments, (Nalbach (1993); Nalbach and Hengstenberg (1994)) it has been shown that flies with cut off halteres are unable to stay aloft in flight and to start their wingbeats. To confirm the role of the halteres, we loaded the halteres with a small drop of glue. We deposited a drop of 0.2 mg to each haltere, equivalent to 1% of the mass of *Episyrphus Balteatus*. We also tested the fly's response to a strong change in the lighting conditions. The flies were illuminated from below with a white halogen light (Kaiser Studiolight H, irradiance of 1.76×10^{-11} $W.m^{2}$). We finally tested whether the righting reflex was driven by head rotation by gluing the head to the thorax. Body and head rotations were recorded using a high-speed video camera (Phantom VEO E310) at a rate of 3600 frames per second (resolution: 1280x800 pixels). A drop of glue (in average 0.2mg with 50% beeswax, 50% rosin) was deposited at the tip of the two halteres in the loaded halteres condition and between the head and the thorax (0.6mg) in the head-thorax glued condition under visual control using an eyepiece-less stereo microscope (Mantis Elite by Vision Engineering) with a magnification of 15. A total number of 13 falls (involving 3 males and 1 female) were recorded with the lighting from below, 11 falls (involving 1 male and 2 females) in the loaded halteres condition and 6 falls (involving 2 females) in the head thorax glued condition. Mean additional mass estimates were performed by loading a piece of paper with 10 drops of glue and calculating the total extra mass divided by 10.

In the loaded halteres condition, the falling flies could be viewed from the side. Projected distance calculations were therefore performed in order to estimate the head and body angles (see supplementary material, figure 1. and Viollet and Zeil (2013)).

Statistical comparisons were performed with R (R Core Team (2019), www.R-project.org) on the experimental variables between the normal condition and the two conditions (lighting from below and loaded halteres condition) with a posthoc Kruskal Dunn test (posthoc.kruskal.dunn.test) and on one variable (time of the righting reflex) between 6 sample of 6 trials of the normal condition and the head-thorax glued condition with a Wilcoxon test (wilcox.test)

RESULTS

After being released upside-down, hoverflies *Episyrphus balteatus*, are able to right themselves as from the first wingbeat by generating a 180° roll rotation via an asymmetric stroke amplitude between the right and left wings defined by the positional angles ϕ_R and ϕ_L shown in figure 2A, respectively. Two phases can be observed during the righting process: the first phase where, in the case of a clockwise rotation, ϕ_L is larger than ϕ_R, followed by the second phase, where ϕ_R becomes larger than ϕ_L (see figure 2A and B). The stroke amplitudes of the two wings recorded during Trial 7 are shown in Figure 2A. Figure 2B shows the occurrence of a smooth transition between the peak-to-peak stroke amplitudes of the left and right wings versus each wingbeat period. It can therefore be concluded that the body rotation results from the difference in stroke amplitude. At the first wingbeat, active torque roll is triggered by the difference between the right and left wing stroke amplitudes, but after five wingbeats, the sign of the difference is reversed, resulting in an active counter

torque roll stabilizing the fly's attitude on the roll axis. As shown in figure 2C, where the thorax angle (θ_{TR}) is plotted versus the normalized wingbeat amplitude difference clearly shows the presence of two clusters. The reversal of the sign of the normalized wingbeat amplitude difference observed during the righting manoeuvre suggests that the torque roll movement is suddenly reversed during the righting process, in line with the occurrence of an aggressive manoeuvre.

Righting was therefore studied here from the first wingbeat to the end of the righting process, defined as the moment when θ_{HB} , the (Head/Body angle) became equal to 0°. As can be seen from figure 3, the amplitude and duration of the righting process were fairly variable. It was observed in some cases that hoverflies kept on rotating after reaching 0° (i.e -90° in Trial 1, see figure 3), while in other cases, they stopped righting before reaching an angle of 0° (i.e., 25° in Trial 12, see figure 3). Despite the disparities observed among the responses, figure 5 shows that the time elapsing before the first wingbeat (median value 23.75ms), the time taken by the hoverflies to reorient themselves (median value 48.8ms), the number of wingbeats (median value 6 wingbeats) and the distance travelled during the righting process(median value 39.6mm) did not vary conspicuously.

As observed in figure 3, a time lag occurred systematically between θ_{HR} (Head Roll angle) and θ_{TR} (Thorax Roll angle): the body initiated the righting response before the head. The maximum value of this time lag was determined by subtracting the time at the minimum value of the head roll angular speed (Ω_{HR}) from the time at the minimum value of the body angular roll speed (Ω_{TR}) (see figure 4). As shown in figures 3 and 5E, the maximum time lag ranged from 9ms to 28ms.

To account for the time lag observed between θ_{HR} and θ_{TR} , it seemed to be worth analysing the dynamics of θ_{HB} . The time lag between θ_{TR} and θ_{HR} resulted from changes in θ_{HB} (figure 3). θ_{TR} rotated first, while θ_{HR} remained constant, resulting in an increase in θ_{HB} from a null value to a maximum value, and θ_{HR} then started to rotate and to catch up with θ_{TR} , resulting in a decrease in θ_{HB} from the maximum value down to null. Disparities were also observed between the 13 trials in the maximum value of θ_{HB} , which ranged from less than 50° (in Trials 4 and 13) to more than 100° (in Trials 7 and 11).

Fast 180° roll rotations performed by hoverflies during the righting process resulted from angular speeds Ω_{HR} and Ω_{TR} as fast as -10 x10^3 °/s (see Trial 2 in the figure 4). Thanks to the low inertia (I_{roll} of 9.76e-12 kg.m^2) and the fast dynamics (48.8ms, see figure 5), a hoverfly can produce fast body angular speeds when required to achieve a complete righting process. The time elapsing between Ω_{HR} and Ω_{TR} is also clearly visible in figure 3: Ω_{TR} started to increase before Ω_{HR} . Two phases can be observed, depending on the value of Ω_{HB} . The hoverfly's righting states and phases are shown in figure 4, where it can be seen that the head rotated first anti-clockwise to compensate for the rotation of the thorax, and then clockwise in order to become realigned with the body.

Previous studies have shown that θ_{HB} is stabilized and compensates for the changes in θ_{TR} (Hengstenberg (1993); Hardcastle and Krapp (2016); Sandeman and Markl (1980)). The best way of compensating quickly for these changes is surely to measure them directly and to use this measurement to compensate for them. We adopted the hypothesis that the time elapsing between θ_{TR} and θ_{HR} might result from the gaze stabilization reflex.

For the three additional experiments shown in figure 6 (Lighting from bellow, loaded halteres and head-thorax glued) hoverflies were always able to right themselves. When lighting from below, flies right themselves in similar short lapse of time (median value 61.11ms) with a shorter time lag (median value 8.1ms, significant differences) and a smaller θ_{HB} (median value 44.19°, significant differences) than the lighting from above condition. When halteres were loaded with glue, flies right themselves faster (median value 29.72ms, significant differences) with a smaller time lag (median value: 6.1ms, extremely significant differences) and a similar θ_{HB} (median value 58.21°). When the head and thorax were glued together no significant difference were found in terms of duration of the righting reflex (median value 44.72ms).

DISCUSSION

In line with previous studies carried out at our laboratory (Goulard et al. (2015; 2016; 2018a;b), hoverflies were dropped under free fall conditions, upside-down with their legs touching the top of the box, in order to study aerial righting in flies for the first time. As expected, hoverflies in the upside-down position were found to trigger their wingbeats and to rotate quickly in order to regain the right-side up position within a short lapse of time (48.8ms, see figure 5C). These rotational manoeuvres involved asymmetric wing strokes (active torque, see figure 2) resulting in fast thorax roll velocities of the order of several thousands of degrees per second (range: -2×10^3 °/s to -12×10^3 °/s see figure 4).

Proprioceptive processes used to detect the upside-down state

In our set-up, hoverflies can probably use two main types of cues when there are held upside-down. Those of the first kind consist of the DLR (Dorsal light response), which is a reflex allowing several families of insects to determine their orientation due to the fact that the brightest part of the environment is presumably located above them (Mittelstaedt (1950); Hengstenberg (1993); Goulard et al. (2015; 2018a); Meyer and Bullock (1977); Schuppe and Hengstenberg (1993)). In a previous experiment, Goulard et al. (Goulard et al. (2018a)) have shown that lighting from below drastically affects hoverflies' stabilisation during free fall, which proves that hoverflies are highly sensitive to light coming from the ground. In the present case, the halogen light projected from below would provide the hoverfly (upside-down) with a vertical reference frame oriented in the appropriate position. Therefore, if the fly's righting process depended only on the DLR, we would observe the occurrence of no righting in this condition, which was never the case. In addition, we observed only a small effect of the lighting conditions on the head movement during the righting process (see figure 6 with a shorter time lag and a smaller θ_{HB}) suggesting that the DLR might be involved in the feedforward control of the head as a modulation of its gain

(see box $F_{NM}(s)$ in figure 7). Further experiments are required to better understand the DLR contribution to the righting reflex.

The cues of the second kind are proprioceptive cues which are sensed by the insect legs' chordotonal organs (Tuthill and Wilson (2016)). The proprioceptive processes involved in insects' postural reflexes are simulated by the weight of the legs (Horn and Lang (1978); Kress and Egelhaaf (2012); Horn (1982)). Force and load signals act as orientation cues (walking - Büschges et al. (2008); Duysens et al. (2000)). Hoverflies are therefore able to quickly estimate the righting posture required to respond to loss of contact between their legs and the substrate (via the tarsal reflex) (see Binns (1977); Fraenkel (1932); Pringle (1938); Dudley (2002)). As suggested in the model presented in figure 7, DLR combined with leg proprioception may be used by flies to estimate the angle of the surface on which they are standing, and would therefore enable them to set the value of the input reference signal *Ref* before taking off from a tilted surface. The input reference signal is an input signal corresponding to the reference value that the closed-loop system tries to reach in steady state. In conclusion, DLR and proprioception are likely to conflict when the lighting originates from below, but further experiments are now required to be able to clearly define their respective contributions to the righting reflex.

Body roll model and righting response

In fruit flies, roll torque results from asymmetric wing movements (Ristroph et al. (2010); Sane (2003); Beatus et al. (2015); Ristroph et al. (2013)), which leads to a difference in the lift generated by each wing. The results on the normal condition as well as in the head-thorax glued condition obtained here tend to confirm that the aerial righting performances of *Episyrphus balteatus* are purely aerodynamic, i.e., hoverflies produce asymmetric flapping movements in order to trigger a torque roll and right themselves (see figure 2). As shown in figure 2 and in the inset of figure 7 (sign of the simulated torque roll signal), two phases exist: the first positive part and the second negative part resulting in the righting process. The active force use to start the rotation of the body (phase 1) seems to be larger than the force used to stabilize it at the end of the righting (phase 2). Point cloud of figure 2C shows clearly two clusters suggesting that a passive torque roll (Hedrick et al. (2016)) related to the friction of the wings also contribute to the stabilization of the fly leading to this asymmetry in the wingbeat amplitude observed during a complete righting process.

It is worth noting that we have never observed any righting manoeuvres involving body pitch rotations under normal condition. Body pitch depends on the fly's ability to shift the center of mass forwards (or backwards) in order to trigger a nose-up (or nose-down) pitch torque movement (Ristroph et al. (2013)). Controlling the wingbeat amplitude differentially is probably much more efficient and direct than using each wingbeat's duty cycle. The duty cycle means the ratio between the durations of the upper (upstroke Θ_{Up}) and lower (downstroke Θ_{Down}) parts of a wingbeat (see figure 2A). As explained in the Introduction, vertebrates are known to move segments of their body, legs (reptiles) or tail (lizards) in certain configurations in order to control the instantaneous moment of inertia and the angular momentum. However, most hoverflies are much smaller than vertebrates and they are exposed to more viscous aerodynamic forces (see Jusufi et al. (2011)). Aerodynamic interactions are therefore likely to predominate over inertial effects. We never observed the occurrence of any righting movements without any wingbeats being triggered and the head-

thorax glued condition showed that the righting is not coupled to any head movement. We therefore modelled the roll dynamics in terms of a purely second order system (a double integrator) receiving torque U_{roll} as its inputs and delivering, via the moment of inertia I_{roll}, outputs specifying the appropriate thorax roll speed Ω_{TR} and thorax roll angle θ_{TR}. No evidence showing the presence of a neural integrator serving to estimate the roll has ever been obtained so far, although the existence of this component is biologically plausible as the temporal drift inherent to any vibrating rate gyro such as the halteres (Acar and Shkel (2009)) is likely to be very small during the short time required to perform righting manoeuvres. Once the righting has been accomplished, hoverflies can count on vision in addition to the thorax roll speed to estimate their body roll and compensate for any drift (see the unbiased rate gyro method based on an inertial measurement unit (Wu et al. (2015))).

Closed-loop roll control during the righting process

Accurate control of the body attitude (roll) during the righting process is also necessary to be able to reach the steady-state 0° position (right side-up) reliably. Flies may use visual motion cues (Meresman et al. (2014); Yanoviak et al. (2010)) combined with inertial measurements provided by the halteres (Dickinson et al. (1999); Fraenkel and Pringle (1938)). During flight, the halteres are known to oscillate up and down in antiphase with the wings (see Nalbach (1993)) and are therefore highly receptive to the state of wing activation (see Dickerson et al. (2019); Parween and Pratap (2015); Deora et al. (2015); Pratt et al. (2017); Deora et al. (2017))

However, due to the extremely short duration of the righting reflex ($\sim$ 49ms) and the relatively long processing time required by the motion processing neurons (about $\sim$ 50ms in the fruit fly, see Warzecha and Egelhaaf (2000); Frye (2009)), the righting reflex can be assumed to depend only on the angular body speed measurements provided by the halteres. The halteres are known to show fast response times of only approximately 5ms (Pringle and Gray (1948); Sandeman and Markl (1980); Taylor and Krapp (2007); Dickinson and Muijres (2016); Sherman and Dickinson (2004; 2003); Liu et al. (2016)), and the righting response times recorded here were consistent with those of the halteres. A self-stabilizing reflex has been studied in fruit flies performing cruising flights (Ristroph et al. (2010; 2013); Beatus et al. (2015)). Upon undergoing an external disturbance, the fly adjusts its body orientation in order to recover its initial side-up position within 30ms. The roll-induced perturbations applied in the latter studies amounted to about 45°. In addition, the halteres are known to be involved in insects' detection of fast perturbations (Ristroph et al. (2010); Dickinson et al. (1999)) and in fruit flies' mediated equilibrium reflexes (Liu et al. (2016); Nalbach (1993; 1994); Nalbach and Hengstenberg (1994); Dickinson et al. (1999); Fox and Daniel (2008); Huston and Krapp (2009); Frye (2009)).

Head/body movements and time lags

Hoverflies are able to rotate their head around the roll axis with respect to their body up to an angle of 77.7° (median value, see figure 5.F.). During the righting phase, we observed a time lag of 16.3ms (median value, see figure 5.E.) between the head and body rotations. The body starts to rotate first, and then the head rotates in the direction imposed by the body. Three possibilities can be envisaged for modelling this time lag:

- as suggested by the results of a previous study on wasps (Viollet and Zeil (2013)), head orientation may be controlled by a feed-forward signal, while a copy of the command signals sent to the wing motoneurons is also sent with the opposite sign to the head position (neck) servo system. If a simple time lag is inserted into the pathway controlling the head orientation, one might wonder what the effects of this time lag might be, and how biologically relevant it might be. Adding a time lag would definitely alter the performances of the gaze stabilization reflex, which plays a crucial role in blowflies (see review Hardcastle and Krapp (2016)).

- as suggested by previous studies on gaze stabilization (see Hardcastle and Krapp (2016); Mittelstaedt (1950)), without any need for halteres, passive inertial stabilization may serve to compensate for body rotations. Assuming the neck to act like a simple spiral spring, the head would first stay behind and then be pulled in the direction of the rotation imposed by the body. However, the difference in mass between body (21mg) and head (5mg), corresponding to a ratio of 4.2 between the head and body moments of inertia (assuming the body to be a cylinder and the head, a sphere) is not consistent with the idea that a purely passive process of stabilization might occur during the righting process. In addition, (Gilbert and Bauer (1998)) has established that in the flesh fly, head posture results from both a passive and an active control of the head based on the prosternal organs. It would certainly be of interest to investigate hoverflies' head dynamics more closely in future studies. Here we modelled the neck motor system in the form of a first order filter (a $F_{NM}(s)$ transfer function) to account for the head's moment of inertia and the friction of the neck muscles. Values of $F_{NM}(s)$ were obtained by fitting the model's response to the 13 trials (see figure 4).

- as shown in figure 8B (and also in the model in figure 7), we assumed that the θ_{HB} is negatively proportional to Ω_{TR} (see block -1 in the model): the head is driven by the body roll speed. The head therefore changes its rotational direction when the body roll speed decreases. Figure 8 shows that the head angle is highly correlated with the peak in the roll angular speed and not correlated with any particular value of the head/body angle. The role of a switch control would be very unclear in terms of its functionality, whereas a direct control of the head based on the body's angular speed makes sense in terms of gaze stabilization reflex.

As suggested by the authors of previous studies on fast haltere-induced compensatory head movements (Hengstenberg (1993); Hardcastle and Krapp (2016); Sandeman and Markl (1980)), the time-lag observed here between the head and body responses may result from the gaze stabilization reflex being activated at the very beginning of the wingbeats. As described in our model (see figures 7), the feedforward control of the head depends on the body's angular speed transmitted by the halteres. As in the simulated response (see figures 8A and 8B), the orientation of the head with respect to the body θ_{HB} is proportional to the body's angular speed Ω_{TR}. The head therefore adopts the opposite response to that of the body. In the first phase, the head compensates for the body rotation while the body speed is increasing, and in the second phase, the head rotates as dictated by the body roll. As indicated by the dashed line in figure 8B, the direction of the head rotation is reversed when the body's angular speed starts to decrease. On the basis of the present model, the existence of a feedforward head control based on the thorax's angular speed suggests that the angular position of the head with respect to the body θ_{HB} must be strongly correlated with the

thorax's angular speed Ω_{TR}. We therefore analyzed the cross-correlation between these two normalized signals (see figure 9A). The cross-correlation function applied to the 13 trials showed the existence of a time lag of 7.5ms (median value, see figure 9D) with a standard deviation as small as 2.5ms, which suggests the existence of a strong correlation between the thorax speed and the head orientation, as was to be expected. In addition, the simulated time lag observed between head and body upon combining a physically plausible closed-loop control of the body roll with a feedforward control of the head orientation accounts accurately for the time lag observed in hoverflies (see figure 8). It is worth noting that the two phases in the simulated head/body movement would require a seamless feedforward control of the head orientation based on the body's angular speed transmitted by the halteres.

Haltere-based feedback and feedforward control systems

As shown by the 3D animation presented in the supplementary data video, the present dynamic model can make a fly rotate by 180° and reach a stable steady-state orientation of 0° within a period of 50ms, which is similar to that recorded in hoverflies' responses (see figure 5C). As shown in figure 8, this dynamic model shows very similar time patterns to hoverflies' average responses, as well as similar roll head/body angles and body angular speeds, which can be as fast as 10×10^3 °/s. Like blowflies, which perform fast body roll rotations of up to 2×10^3 °/s (Schilstra and Hateren (1999)) with a maximum amplitude of $\pm 90°$ (Hengstenberg (1988)) and Bembix wasps, which can perform extremely pronounced body roll movements with an amplitude of up to 180° at 2-4 $\times 10^3$ °/s (Zeil et al. (2008)), *Epysirphus Balteatus* hoverflies are another example of outstandingly fast fliers. During the high-speed rotations recorded during the righting process, the role of vision in the flight stabilization process will presumably be very small, while that of the halteres, which, with a very small latency, concomitantly deliver a feedback-loop signal stabilizing the body's roll (see fruitfly Beatus et al. (2015)) and a fast feedforward signal (lasting about 3-5ms in blowflies, Sandeman and Markl (1980); Hengstenberg (1993)) which may serve to adjust the head orientation. However, one might wonder why it is necessary for the fly to activate its gaze stabilization reflex during the righting manoeuver. The model presented here suggests that compensatory head movements may occur as soon as the body starts to rotate at the onset of the wingbeats, which means that the halteres are also activated (Nalbach (1993)). To check whether the time lag observed between the head and body resulted from head roll control by the halteres, we loaded the haltere with a drop of glue (see Material and Methods section). The additional mass significantly shortened the time lag (median value: 6.1ms) than under normal conditions or with lighting from below. We also observed a significant effect of this extra mass on the rotational dynamics, since the insects took a shorter time to rotate, which is in line with the occurrence of an increase in the maximum body angular speed, which could be as fast as 25.84×10^3 °/s in comparison with 9.502×10^3 °/s under normal conditions. However, a conspicuous behavioural difference was also observed not only on roll but also on pitch manoeuvres. By adding a mass at the tip of each haltere, we increased the mass moment of inertia and thus decreased the haltere's natural frequency in both the actuation and sensing directions (see Parween and Pratap (2015)). This also increased the sensitivity (gain) of the halteres to the Coriolis force (see Wu et al. (2002); Northrop (2000)). In addition, as shown by (Parween et al. (2014)), periodic temporal strain variations due to the Coriolis force occur at the same frequency in both pitch and roll movements (while also showing the same harmonics) but differ in terms of their amplitude. By increasing the mass, we probably increased the coupling existing between the pitch and roll perceived, degrading the fly's ability to stabilize its pitch and roll movements efficiently. Greater body rotational speeds

may also have been caused by a change in the haltere gain. Lastly, in their study on mosquitoes, Dickerson et al. have shown that a change of just a few nanograms in the mass of the halteres can lead to unstable flight performances (see Dickerson et al. (2015)). Adding a few milligrams to the hoverfly's halteres decreases the value of the haltere's lateral resonant frequency ω (in rad/s) defined as follows (see Wu et al. (2002)):

$$\omega = \sqrt{\frac{k_l}{m}} \tag{1}$$

where k_l is the lateral stiffness and m is the mass of the haltere. As consequence, increasing m certainly drastically affects the closed-loop control of the fly's body dynamics, resulting in the considerable instability we observed during the righting process.

As discussed by Taylor and Krapp (Taylor and Krapp (2007)) and recently by Hardcastle and Krapp (Hardcastle and Krapp (2016)), gaze stabilization is crucial to steady flight because it reduces motion blur. It would therefore not be surprising if the gaze stabilization reflex was activated at a very early stage during the righting maneuvers once the wingbeats have been triggered and the halteres are therefore vibrating as well. It is worth noting that gaze stabilization is not detrimental to the fly's ability to start rotating within a very short time. A righting response lasting for about 50ms might suffice to enable the gaze stabilization reflex to be fully operational during the subsequent cruise flight.

Acknowledgements

We are most grateful to Julien Diperi for his contribution to building the experimental set-up and to Marc Boyron for developing the electronics: all the research presented in this paper was based on their work. We also want to thank Jessica Blanc for correcting and improving the English manuscript.

Competing interests

We have no competing interests to declare.

Contribution

A.V. designed and conducted the experiments, analysed the data, developed the model, carried out the analyses and drafted the manuscript; L.V.-P. and J.-L.V. helped to develop the model and to draft the manuscript. S.V. helped to design the experiment and develop the model, coordinated the study and helped to draft the manuscript.

Funding

We acknowledge support from the Centre National de la Recherche Scientifique (CNRS), Aix-Marseille Universite and the Agence Nationale de la Recherche (ANR) (in the framework of the OrigaBot project ANR-18-CE33-0008-01).

Ethics

No ethical authorization for animal research or permission to carry out fieldwork were required for this study.

REFERENCES

Acar, C. and Shkel, A. (2009). MEMS Vibratory Gyroscopes: Structural Approaches to Improve Robustness. *Springer US*.

Beatus, T., Guckenheimer, J. M., and Cohen, I. (2015). Controlling roll perturbations in fruit flies. *Journal of The Royal Society Interface*, 12(105).

Binns, E. S. (1977). Take-off and the 'tarsal reflex' in Aphis fabae. *Physiological Entomology*, 2(2):97–102.

Büschges, A., Akay, T., Gabriel, J. P., and Schmidt, J. (2008). Organizing network action for locomotion: Insights from studying insect walking. *Brain Research Reviews*, 57(1):162–171.

Deora, T., Gundiah, N., and Sane, S. P. (2017). Mechanics of the thorax in flies. *Journal of Experimental Biology*, 220(8):1382–1395.

Deora, T., Singh, A. K., and Sane, S. P. (2015). Biomechanical basis of wing and haltere coordination in flies. *Proceedings of the National Academy of Sciences*, 112(5):1481–1486.

Dickerson, A. K., Shankles, P. G., Berry, B. E., and Hu, D. L. (2015). Fog and dense gas disrupt mosquito flight due to increased aerodynamic drag on halteres. *Journal of Fluids and Structures*, 55:451–462.

Dickerson, B. H., de Souza, A. M., Huda, A., and Dickinson, M. H. (2019). Flies Regulate Wing Motion via Active Control of a Dual-Function Gyroscope. *Current Biology*, 29(20):3517–3524.

Dickinson, M. and Muijres, F. (2016). The aerodynamics and control of free flight manoeuvres in Drosophila. *Philosophical Transactions of the Royal Society B: Biological Sciences*, 371(1704).

Dickinson, M. H., Lehmann, F.-O., and Sane, S. P. (1999). Wing Rotation and the Aerodynamic Basis of Insect Flight. *Science*, 284(5422):1954–1960.

Dudley, R. (2002). The Biomechanics of Insect Flight: Form, Function, Evolution. *Princeton University Press*.

Duysens, J., Clarac, F., and Cruse, H. (2000). Load-Regulating Mechanisms in Gait and Posture: Comparative Aspects. *Physiological Reviews*, 80(1):83–133.

Egelhaaf, M. (2002). Neural encoding of behaviourally relevant visual-motion information in the fly. *Trends in Neurosciences*, 25(2):96–102.

Fox, J. L. and Daniel, T. L. (2008). A neural basis for gyroscopic force measurement in the halteres of Holorusia. *Journal of Comparative Physiology A*, 194(10):887–897.

Fraenkel, G. (1932). Untersuchungen über die Koordination von Reflexen und automatisch-nervösen Rhythmen bei Insekten. *Zeitschrift für vergleichende Physiologie*, 16(2):418–443.

Fraenkel, G. and Pringle, J. W. S. (1938). Biological Sciences: Halteres of Flies as Gyroscopic Organs of Equilibrium. *Nature*, 141(3577):919–920.

Frye, M. A. (2009). Neurobiology: Fly Gyro-Vision. *Current Biology*, 19(24):1119–1121.

Gilbert, C. and Bauer, E. (1998). Resistance reflex that maintains upright head posture in the fresh fly Neobellieria bullata (Sarcophagidae). *The Journal of experimental biology*,10(19):2735–2744.

Goulard, R., Julien-Laferriere, A., Fleuriet, J., Vercher, J.-L., and Viollet, S. (2015). Behavioural evidence for a visual and proprioceptive control of head roll in hoverflies (Episyrphus balteatus). *Journal of Experimental Biology*, 218(23):3777–3787.

Goulard, R., Verbe, A., Vercher, J.-L., and Viollet, S. (2018a). Role of the light source position in freely falling hoverflies' stabilization performances. *Biology Letters*, 14(5).

Goulard, R., Vercher, J.-L., and Viollet, S. (2016). To crash or not to crash: how do hoverflies cope with free-fall situations and weightlessness? *The Journal of Experimental Biology*, 219(16):2497–2503.

Goulard, R., Vercher, J.-L., and Viollet, S. (2018b). Modeling visual-based pitch, lift and speed control strategies in hoverflies. *PLOS Computational Biology*, 14(1).

Hardcastle, B. and Krapp, H. (2016). Evolution of Biological Image Stabilization. *Current Biology*, 26(20):1010–1021.

Hedrick, T.L. and Cheng, B. and Deng, X. (2009). Wingbeat time and the scaling of passive rotational damping in flapping flight. *Science (New York, N.Y.)*, 324:252–255.

Hengstenberg, R. (1988). Mechanosensory control of compensatory head roll during flight in the blowfly Calliphora erythrocephala Meig. *Journal of Comparative Physiology A*, 163(2):151–165.

Hengstenberg, R. (1993). Multisensory control in insect oculomotor systems. *Rev. Oculomot. Res*, 5:285–298.

Hengstenberg, R. (1998). Biological sensors: Controlling the fly's gyroscopes. *Nature*, 392(6678):757–758.

Hengstenberg R., Sandeman D. C., Hengstenberg B., and Horridge George Adrian (1986). Compensatory head roll in the blowfly Calliphora during flight. *Proceedings of the Royal Society of London. Series B. Biological Sciences*, 227(1249):455–482.

Horn, E. (1982). Gravity reception in the walking fly, Calliphora erythrocephala: Tonic and modulatory influences of leg afferents on the head position. *Journal of Insect Physiology*, 28(8):713–721.

Horn, E. and Lang, H. G. (1978). Positional head reflexes and the role of the prosternal organ in the walking fly,Calliphora erythrocephala. *Journal of comparative physiology*, 126(2):137–146.

Huston, S. J. and Krapp, H. G. (2009). Nonlinear Integration of Visual and Haltere Inputs in Fly Neck Motor Neurons. *Journal of Neuroscience*, 29(42):13097–13105.

Jusufi, A., Zeng, Y., Full, R. J., and Dudley, R. (2011). Aerial Righting Reflexes in Flightless Animals. *Integrative and Comparative Biology*, 51(6):937–943.

Kane, T. and Scher, M. (1969). A dynamical explanation of the falling cat phenomenon. *International Journal of Solids and Structures*, 5(7):663–670.

Kress, D. and Egelhaaf, M. (2012). Head and body stabilization in blowflies walking on differently structured substrates. *Journal of Experimental Biology*, 215(9):1523–1532.

Liu, H., Ravi, S., Kolomenskiy, D., and Tanaka, H. (2016). Biomechanics and biomimetics in insect-inspired flight systems. *Phil. Trans. R. Soc. B*, 371(1704).

Liu, P., Sane, S. P., Mongeau, J.-M., Zhao, J., and Cheng, B. (2019). Flies land upside down on a ceiling using rapid visually mediated rotational maneuvers. *Science Advances*, 5(10):eaax1877.

Magnus, R. K. (1924). Experimentell-Physiologische Untersuchungen über die Einzelnen bei der Körperstellung in Tätigkeit Tretenden Reflexe, über ihr Zusammenwirken und ihre Störungen. *Gildemeister M, editor. Monographien aus dem Gesamtgebiet der Physiologie der Pflanzen un der Tiere*, pages 228–459. BerlinSpringer.

Marey, E. (1894). Des mouvements que certains animaux exécutent pour retomber sur leurs pieds, lorsqu'ils sont précipités d'un lieu élevé. *CR Acad. Sci.*, 119:714–717.

Marsden, J. E. and Ostrowski, J. (1998). Symmetries in Motion: Geometric Foundations of Motion Control. In *Motion, Control, and Geometry: Proceedings of a Symposium*, pages 3–19. National Academies Press.

Meresman, Y., Ribak, G., Weihs, D., and Inbar, M. (2014). The stimuli evoking the aerial-righting posture of falling pea aphids. *Journal of Experimental Biology*, 217(19):3504–3511.

Meyer, D. L. and Bullock, T. H. (1977). The hypothesis of sense-organ-dependent tonus mechanisms : history of a concept. *Annals of the New York Academy of Sciences*, 290(1 Tonic Function):3–17.

Mittelstaedt, H. (1950). Physiologie des Gleichgewichtssinnes bei fliegenden Libellen. *Zeitschrift für vergleichende Physiologie*, 32(5):422–463.

Mohren, T. L., Daniel, T. L., Eberle, A. L., Reinhall, P. G., and Fox, J. L. (2019). Coriolis and centrifugal forces drive haltere deformations and influence spike timing. *Journal of The Royal Society Interface*, 16(153).

Mou, X. L., Liu, Y. P., and Sun, M. (2011). Wing motion measurement and aerodynamics of hovering true hoverflies. *Journal of Experimental Biology*, 214(17):2832–2844.

Nalbach, G. (1993). The halteres of the blowfly Calliphora. *Journal of Comparative Physiology A: Neuroethology, Sensory, Neural, and Behavioral Physiology*, 173(3):293–300.

Nalbach, G. (1994). Extremely non-orthogonal axes in a sense organ for rotation: Behavioural analysis of the dipteran haltere system. *Neuroscience*, 61(1):149–163.

Nalbach, G. and Hengstenberg, R. (1994). The halteres of the blowfly Calliphora. *Journal of Comparative Physiology A*, 175:695–708.

Northrop, R. B. (2000). Introduction to Dynamic Modeling of Neuro-Sensory Systems. *CRC Press*.

Parween, R. and Pratap, R. (2015). Modelling of soldier fly halteres for gyroscopic oscillations. *Biology Open*, 4(2):137–145.

Parween, R., Pratap, R., Deora, T., and Sane, S. P. (2014). Modeling Strain Sensing by the Gyroscopic Halteres, in the Dipteran Soldier Fly, Hermetia illucens. *Mechanics Based Design of Structures and Machines*, 42(3):371–385.

Pellis, S. M., Pellis, V. C., and Teitelbaum, P. (1991). Air righting without the cervical righting reflex in adult rats. *Behavioural Brain Research*, 45(2):185–188.

Pratt, B., Deora, T., Mohren, T., and Daniel, T. (2017). Neural evidence supports a dual sensory-motor role for insect wings. *Proceedings of the Royal Society B: Biological Sciences*, 284(1862).

Pringle, J. W. S. (1938). Proprioception In Insects: II. The Action Of The Campaniform Sensilla On The Legs. *Journal of Experimental Biology*, 15(1):114–131.

Pringle, J. W. S. and Gray, J. (1948). The gyroscopic mechanism of the halteres of Diptera. *Philosophical Transactions of the Royal Society of London. Series B, Biological Sciences*, 233(602):347–384.

Ribak, G., Gish, M., Weihs, D., and Inbar, M. (2013). Adaptive aerial righting during the escape dropping of wingless pea aphids. *Current Biology*, 23(3).

Ristroph, L., Bergou, A., Ristroph, G., Coumes, K., Berman, G., Guckenheimer, J., Wang, J., and Cohen, I. (2010). Discovering the flight autostabilizer of fruit flies by inducing aerial stumbles. *Proceedings of the National Academy of Sciences*, 107(11):4820–4824.

Ristroph, L., Ristroph, G., Morozova, S., Bergou, A. J., Chang, S., Guckenheimer, J., Wang, Z. J., and Cohen, I. (2013). Active and passive stabilization of body pitch in insect flight. *Journal of The Royal Society Interface*, 10(85).

Sandeman, D. C. and Markl, H. (1980). Head Movements in Flies (Calliphora) Produced by Deflexion of the Halteres. *Journal of Experimental Biology*, 85(1):43–60.

Sane, S. P. (2003). The aerodynamics of insect flight. *Journal of Experimental Biology*, 206(23):4191–4208.

Schilstra, C. and Hateren, J. H. (1999). Blowfly flight and optic flow. I. Thorax kinematics and flight dynamics. *Journal of Experimental Biology*, 202(11):1481–1490.

Schuppe, H. and Hengstenberg, R. (1993). Optical properties of the ocelli of Calliphora erythrocephala and their role in the dorsal light response. *Journal of Comparative Physiology A*, 173(2):143–149.

Sherman, A. and Dickinson, M. H. (2003). A comparison of visual and haltere-mediated equilibrium reflexes in the fruit fly Drosophila melanogaster. *Journal of Experimental Biology*, 206(2):295–302.

Sherman, A. and Dickinson, M. H. (2004). Summation of visual and mechanosensory feedback in Drosophila flight control. *Journal of Experimental Biology*, 207(1):133–142.

Taylor, G. K. and Krapp, H. G. (2007). Sensory Systems and Flight Stability: What do Insects Measure and Why? *Advances in Insect Physiology*, volume 34, pages 231–316. Elsevier.

Tuthill, J. and Wilson, R. (2016). Mechanosensation and Adaptive Motor Control in Insects. *Current Biology*, 26(20):1022–1038.

Viollet, S. and Zeil, J. (2013). Feed-forward and visual feedback control of head roll orientation in wasps (Polistes humilis, Vespidae, Hymenoptera). *Journal of Experimental Biology*, 216(7):1280–1291.

Wang, Z. J. (2005). Dissecting Insect Flight. *Annual Review of Fluid Mechanics*, 37(1):183–210.

Warzecha, A.-K. and Egelhaaf, M. (2000). Response latency of a motion-sensitive neuron in the fly visual system: dependence on stimulus parameters and physiological conditions. *Vision Research*, 40(21):2973–2983.

Wu, J., Wang, D., and Zhang, Y. (2015). Aerodynamic Analysis of a Flapping Rotary Wing at a Low Reynolds Number. *AIAA Journal*, 53(10):2951–2966.

Wu, W., Wood, R., and Fearing, R. (2002). Halteres for the micromechanical flying insect. *IEEE*. volume 1, pages 60–65 vol.1.

Wystrach, A. and Graham, P. (2012). What can we learn from studies of insect navigation? *Animal Behaviour*, 84(1):13–20.

Yanoviak, S. P., Munk, Y., Kaspari, M., and Dudley, R. (2010). Aerial manoeuvrability in wingless gliding ants (Cephalotes atratus). *Proceedings of the Royal Society B: Biological Sciences*, 277(1691):2199–2204.

Zeil, J., Boeddeker, N., and Hemmi, J. M. (2008). Vision and the organization of behaviour. *Current Biology*, 18(8):R320–R323.

Zeng, Y., Lam, K., Chen, Y., Gong, M., Xu, Z., and Dudley, R. (2017). Biomechanics of aerial righting in wingless nymphal stick insects. *Interface Focus*, 7(1).

Figures

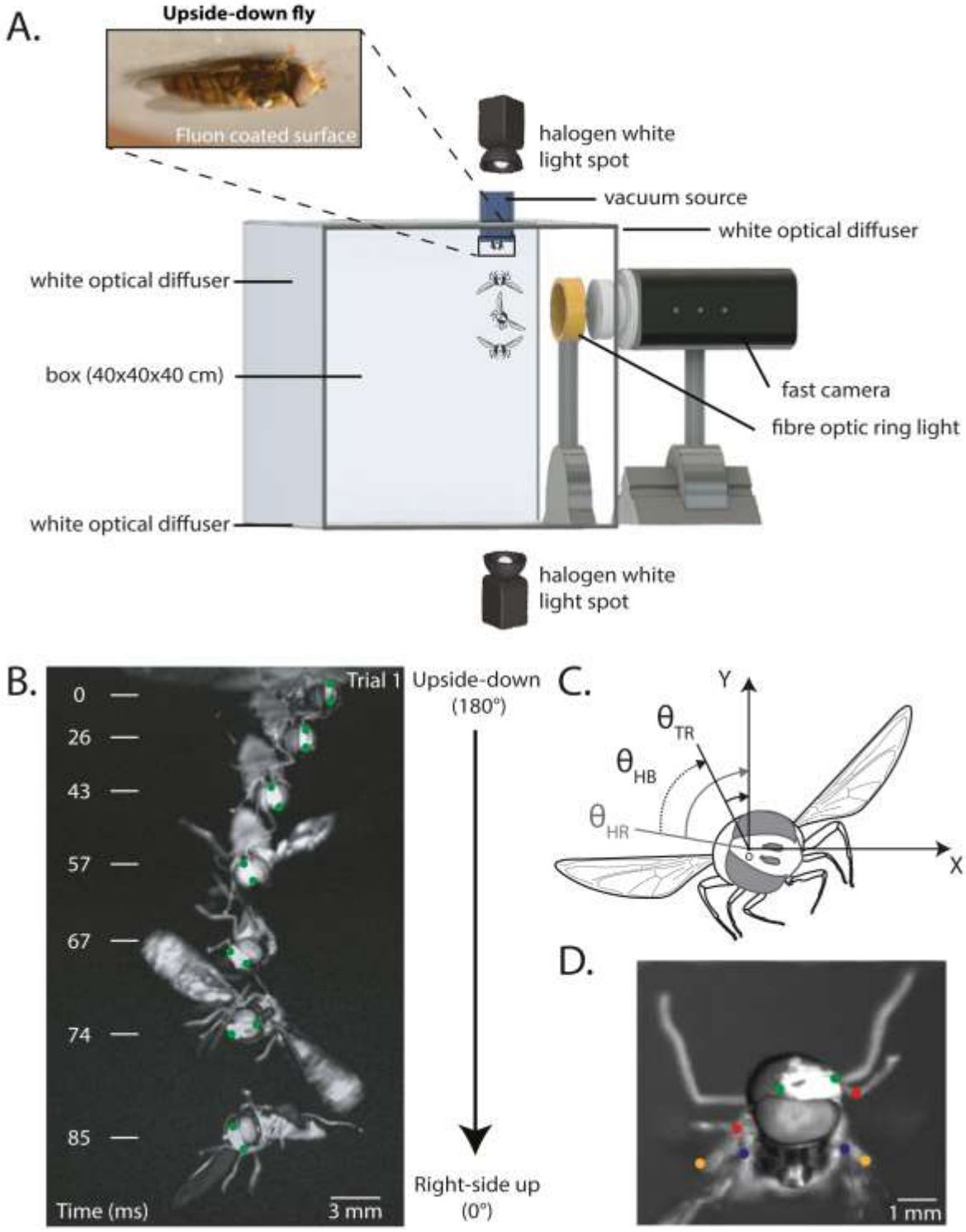

Fig. 1. Illustration of the Aerial righting reflex and the tracking process. A. The experimental set-up used to analyse hoverflies' aerial righting reflex. The observation cage consisted of a 40x40x40 cm transparent PVC box covered with a white diffuser, illuminated from above or below by a halogen light, and from the side by an optic fibre ring light placed around the camera lens. The fly was held upside-down on the ceiling of this box by means of a small capillary tube connected to a vacuum pump. When the vacuum source was turned off, the fly was released and started falling. The fall was recorded with a high-speed video camera equipped with a macro lens operating at a rate of 1600 fps in the full sensor resolution mode (1280x800 pixels). B. A typical

aerial righting reflex sequence recorded. Here we can see a series of body and head rotations making the fly reorient itself dorsoventrally from the upside-down position to the right side up position, corresponding to roll angles of 180° and 0°, respectively. Green points indicate the top and bottom positions of the head tracked. Time frame (in ms) is indicated in the case of each fly's orientation performances. C. Head and body angle relative to the absolute frame: Head (θ_{HR}), thorax (θ_{TR}). Head/body angle (θ_{HB}) is defined in the fly's frame. Angles are defined relative to the vertical. The angle θ_{HB} was calculated using the following equation: $\theta_{HB} = \theta_{HR} - \theta_{TR}$.

D. **Tracking procedure.** To estimate the hoverflies' body orientation, 3 pairs of points were tracked: the junctions between two pairs of forelegs and hindlegs (hindlegs in orange and forelegs in red) and the junctions between the wings and the body (in blue). The orientation of the head was measured based on the top and bottom dots (the green dots marked on the head).

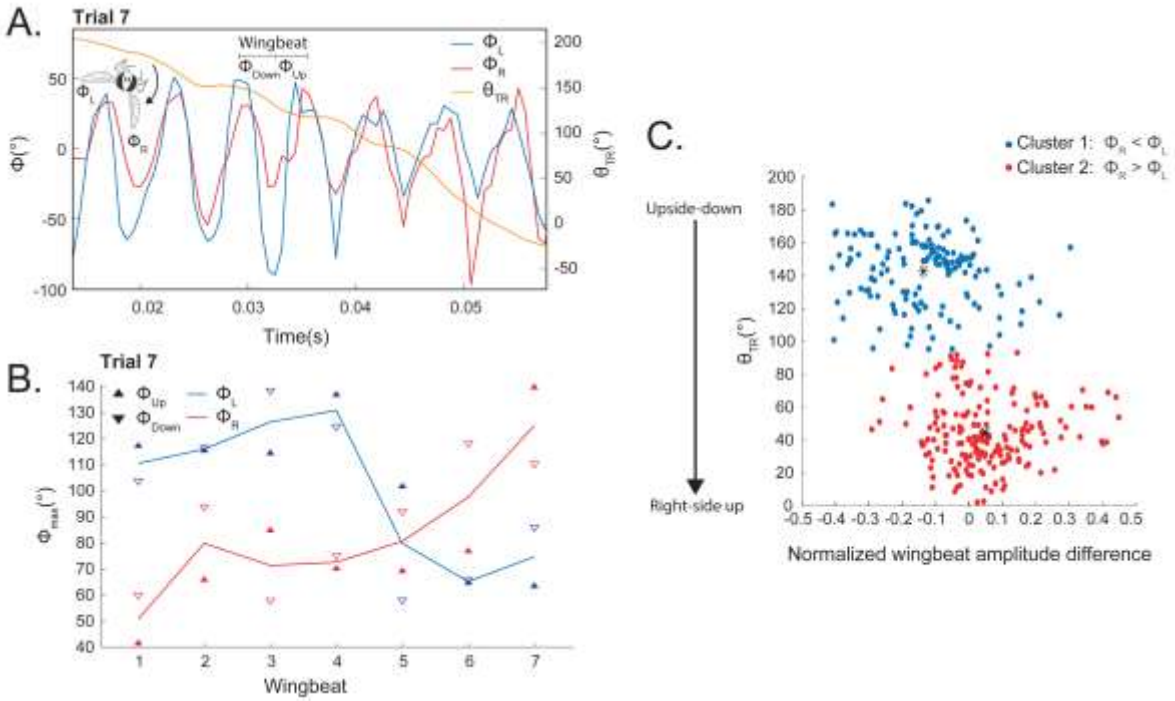

Fig. 2. Wing kinematics on the roll axis. A. Stroke amplitude (positional angle) ϕ with time of the two wings during one clockwise rotation: right wing (ϕ_R in red) and left wing (ϕ_L in blue). Body roll angle θ_{TR} in orange. B. Peak to peak stroke amplitude recorded in one trial. Up and down strokes are differentiated (by arrows pointing upwards and downwards, respectively). Lines correspond to the mean value of the up and down stroke amplitudes in the case of each wingbeat. C. θ_{TR} versus normalized difference in wingbeat amplitude $=$ (ϕ_R - ϕ_L)/180, during 6 trails (Trails 3,5,6,7,10 and 12). Two clusters were found to exist, giving a bss/tss between the sum of squares/total sum of squares) of 85.1 %.

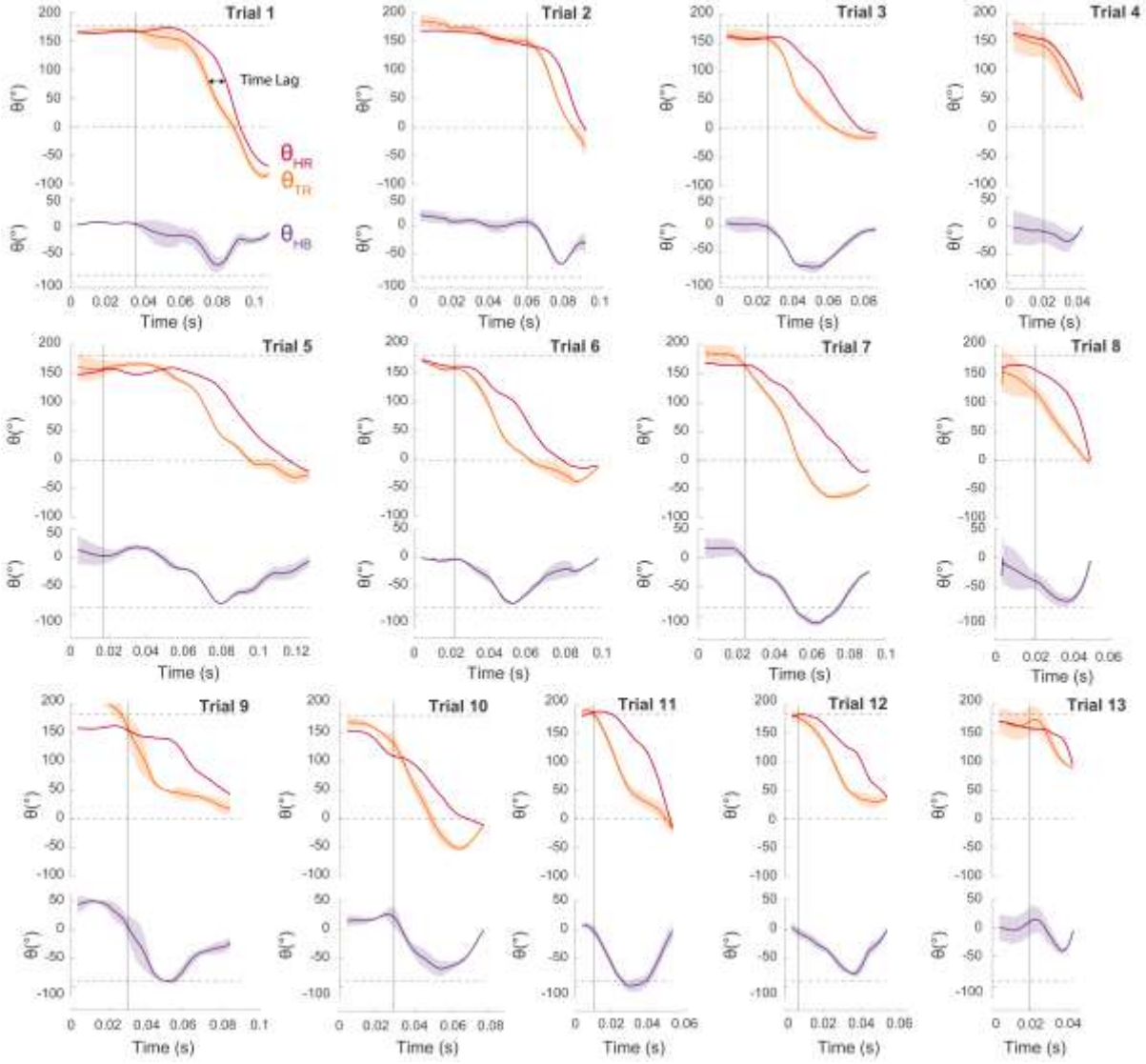

Fig. 3. Plots of head, body and head/body angle (θ_{HR} , θ_{TR} and θ_{HB}) with time in the hoverfly *Episyrphus balteatus*. Right-side up and upside-down positions correspond to roll angles of 0° and 180°, respectively. Thick lines are means and coloured lines are means +- SDs. The SD in θ_{TR} and θ_{HB} was due to the differences between the 3 body tracking methods used (see Methods: hindleg, foreleg and wing junctions). The solid vertical line indicates the time of the first wingbeat and the dotted horizontal dotted lines indicate the angles 180°, 0° and -90°.

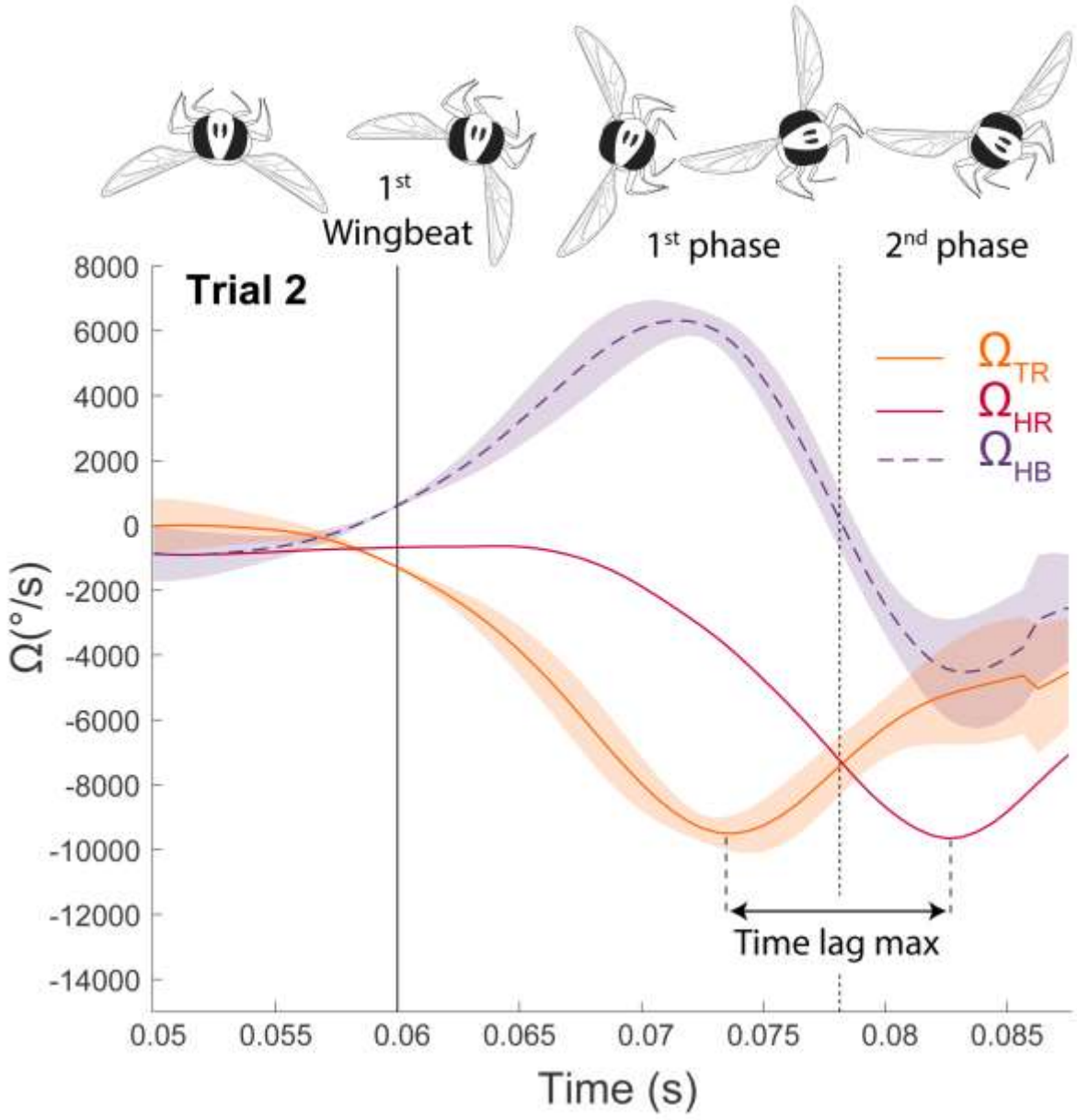

Fig. 4. Dynamic analysis of the insects' righting performances. Illustration of the various phases in the righting process and the roll angular speeds of the thorax (Ω_{TR}), head (Ω_{HR}) and head/body (θ_{HB}) versus time in one trial. The lines correspond to the mean value obtained with the 3 tracking methods used (hindleg, foreleg and wing junctions, see tracking methods) and the transparent areas, to the standard deviations. The solid vertical line corresponds to the first wingbeat and the dotted vertical line marks the border between the two righting phases. Maximum time lag between the head and body corresponds to the time lag between the two peak angular speeds.

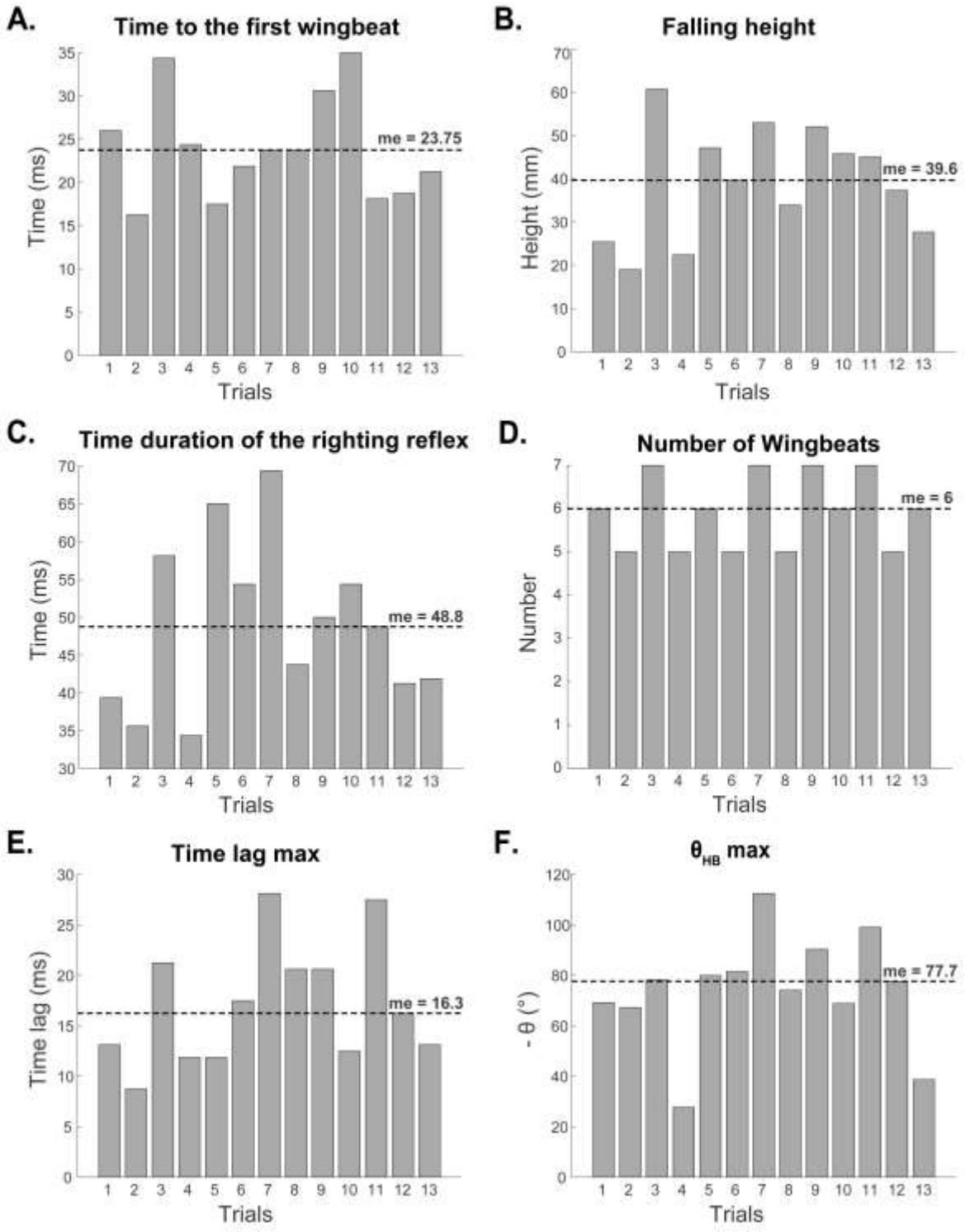

Fig. 5. Aerial righting reflex variables recorded with *Episyrphus balteatus* in each of the 13 trials A. Time duration to the first wingbeat. B. Falling height. C. Time duration of the aerial righting reflex. D. Number of wingbeats. E. Maximum time lag between θ_{HR} and θ_{TR} and F. Maximum value of θ_{HB}. Median value is indicated by the horizontal dotted line and the value me.

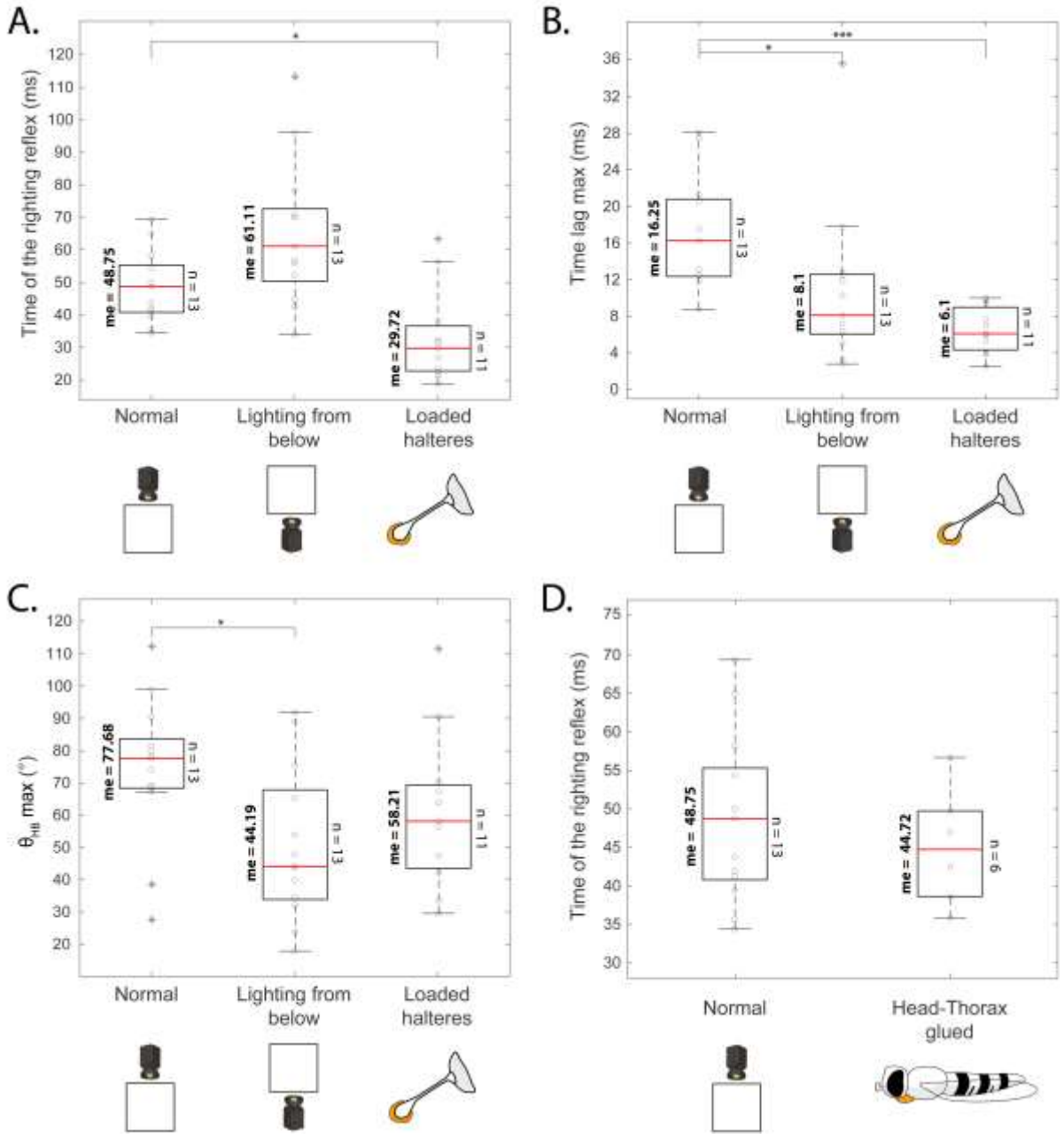

Fig. 6. [A-C] Boxplot comparisons on 3 variables under normal conditions and two of the conditions tested (lighting from below and loaded halteres). A. Time of the onset of the righting reflex (ms), B. Max time lag (ms), C. θ_{HB} max (°). D. Time of the onset of the righting reflex (ms) under normal conditions and head-thorax glued condition. Significance code: *** p-value < 0.001, ** p-value < 0.01, * p-value < 0.05. n indicates the sample size and me indicates the median value.

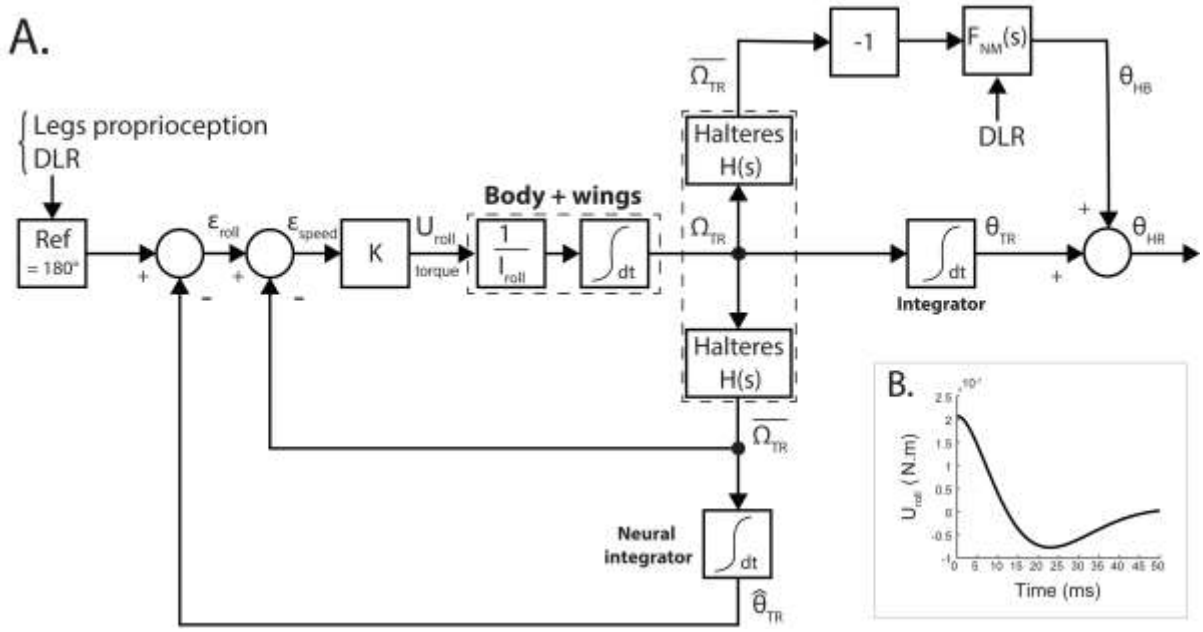

Fig. 7. A. Control block diagram including two nested feedback-loops: the one fast feedback-loop controls the roll angular speed measured by the halteres, and the other, slower loop controls the roll angle on the basis of the estimated $\hat{\theta}_{TR}$ provided by a neural integrator. A feedforward controller $F_{NM}(s) = \frac{k}{\tau_1 s + 1}$ receives the roll speeds measured as it inputs $\overline{\Omega_{TR}}$ and delivers output signals which control the orientation of the head with respect to the body θ_{HB}. The latter signal is therefore proportional to the body roll speed measured $\overline{\Omega_{TR}}$, but with the opposite sign (block -1). The reference input signal Ref controls the amplitude of the body roll. The value of Ref can be set, based on the leg proprioceptive cues and the dorsal light response (DLR). We differentiated between the angular speed of the thorax Ω_{TR} and the speed measured by the halteres, which was expressed as follows: $\overline{\Omega_{TR}}$. For the sake of clarity, the haltere block was split into two identical blocks. $H(s) = \frac{1}{\tau_2 s + 1}$. ϵ_{roll} and ϵ_{speed} are error signals, K is a gain and U_{roll} is the torque roll. B. Typical time course of the simulated control input signal U_{roll} corresponding to torque roll.

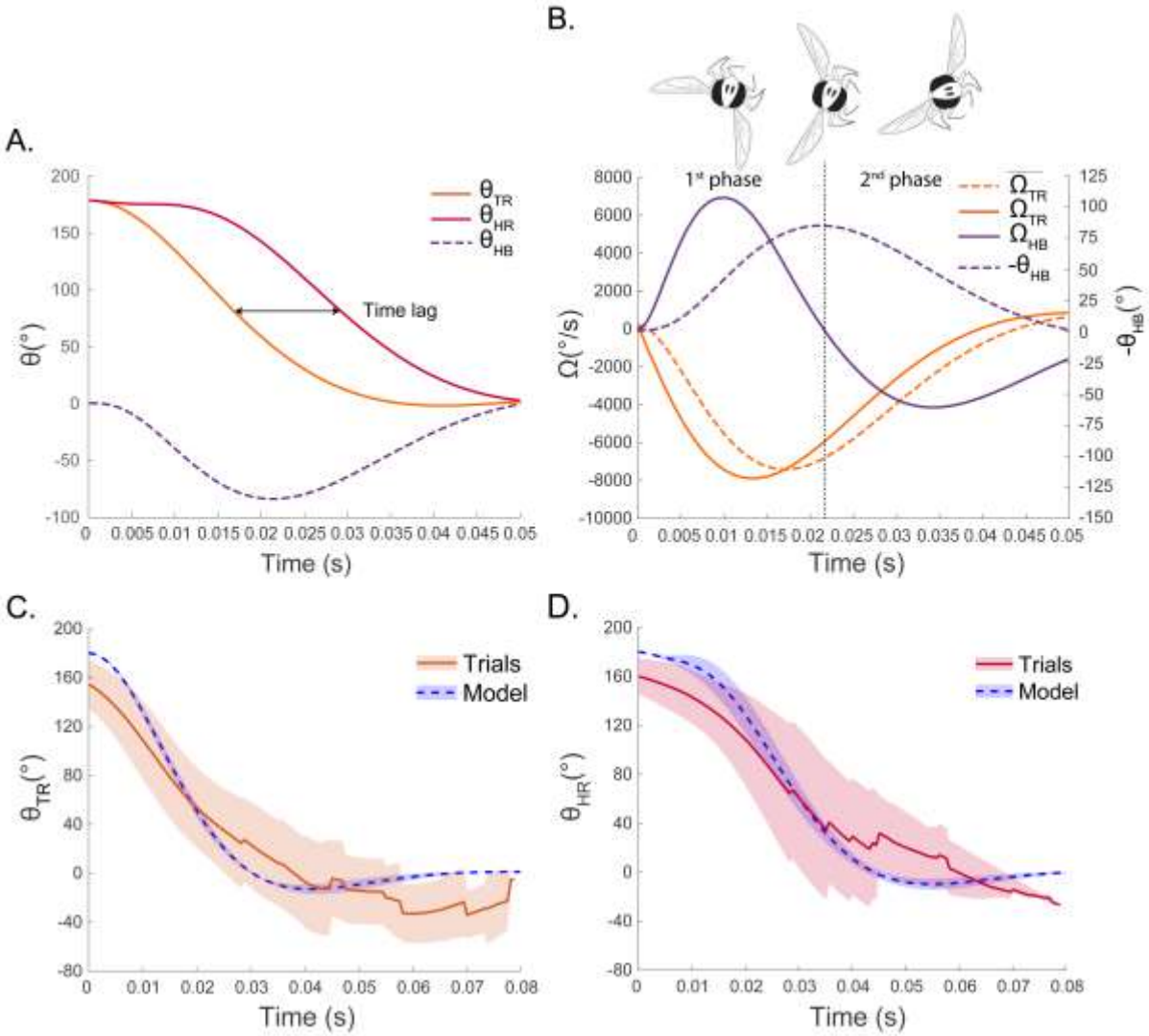

Fig. 8. Response of the righting reflex model. A. Response of θ_{TR}, θ_{HR} and θ_{HB} versus time to a reference input signal Ref = 180°. The model accounts for the time lag observed (see figure 5E) between head and body. B. Main angular speeds and head/body orientation were plotted versus time in order to explain the time lag observed during the roll manoeuver. Due to the feedforward control system (see figure 7), the head/body orientation θ_{HB} can be seen to have faithfully followed the changes in the body's angular speed measured $\overline{\Omega_{TR}}$, taking the opposite sign (-1 block in the model). θ_{HB} is driven by the body roll speed. The head therefore compensates for the body rotation (in the first phase) and then rotates in the same direction as the body (in the second phase) when the sign of the head speed becomes negative at the instant indicated by the vertical dashed lines. Model parameters: Ref = 180°, $K = 1.22e-9$, I_{roll} = 9.76e-12 $kg.m^2$, $H(s) = \frac{1}{0.0035s+1}$, $F_{NM}(s) = \frac{0.012}{0.004s+1}$ .Model parameters were defined by fitting the model to the data recorded in the 13 trials previously performed (see figure 4). **Comparison between data obtained with the model (dotted line) and in the 13 trials (solid line): θ_{TR} (C.) and θ_{HR} (D.).** The same model parameters as previously with K variations (9.760 x10^{-10}, 1.098 x10^{-09}, 1.220 x10^{-09}), $F_{NM}(s)$ variations (8.5 x10^{-3}, 10 x10^{-3}, 13 x10^{-3}) and U_{roll} variation (3.5 x10^{-3}, 4 x10^{-3}, 5 x10^{-3}). Thick lines are means and coloured areas are means +- SDs. Standard deviations were due to K, $F_{NM}(s)$ and U_{roll} variations.

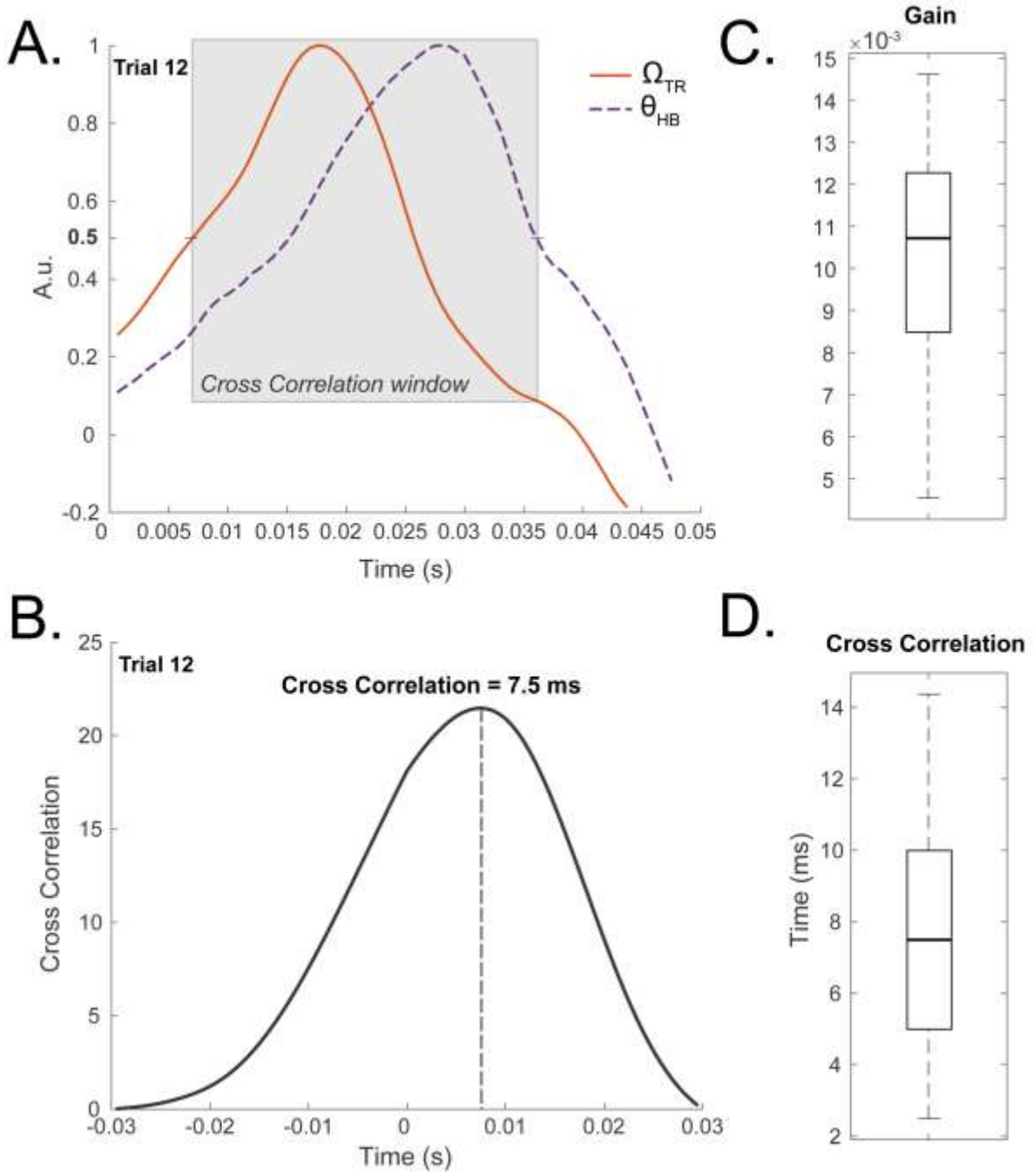

Fig. 9. Cross correlation and Gain. A. Normalised Ω_{TR} and θ_{HB} for one trial. Cross correlation of normalised Ω_{TR} and θ_{HB} was calculated within the temporal window (grey shaded area) starting when increasing Ω_{TR} is higher than 0.5 and ending when θ_{HB} is lower than 0.5. The same threshold of 0.5 was applied for each trial. Result of the cross correlation between the two normalised Ω_{TR} and θ_{HB} for the trial 12 shown in B. and for the 13 trials in C. Gain $= \frac{max(\theta_{HB})}{max(\Omega_{TR})}$ in each trial. Gain of $F_{NM}(s)$ of the model (see figure 8). D. Results of the cross correlations in the 13 trials suggesting the existence of a strong correlation between Ω_{TR} and θ_{HB}.

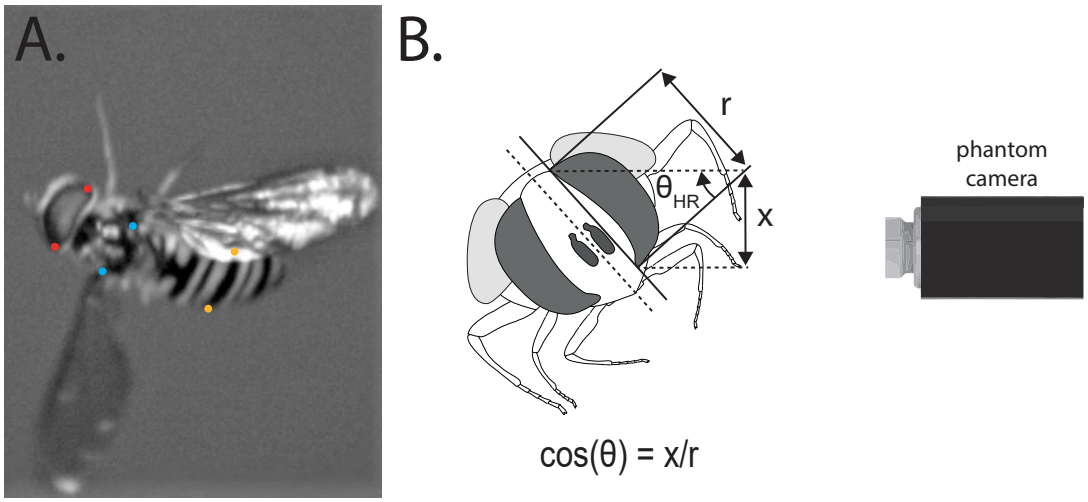

Figure 1: **Estimation of the body roll from a side view of the fly).** A. Body and head orientation. The following pairs of points were tracked: to track the head, the height of the eye was used - top and bottom point (right or left depending on the orientation toward the camera, in red) and to track the body, the length of the body color strip - right and left point (in yellow) or the wing junction (in blue)were used. B. Method of roll angle estimation via projected measurements. The horizontal distance (x, projected distance), along with independent measurements of the length of the fly's long axis (r, real distance) were used to estimate the roll axis orientation (θ) : $Cos(\theta) = x/r$. Visual length measurements selected from each image (projected distance x) and the height of the eye (known distance r) were used to estimate (θ_{HR}).

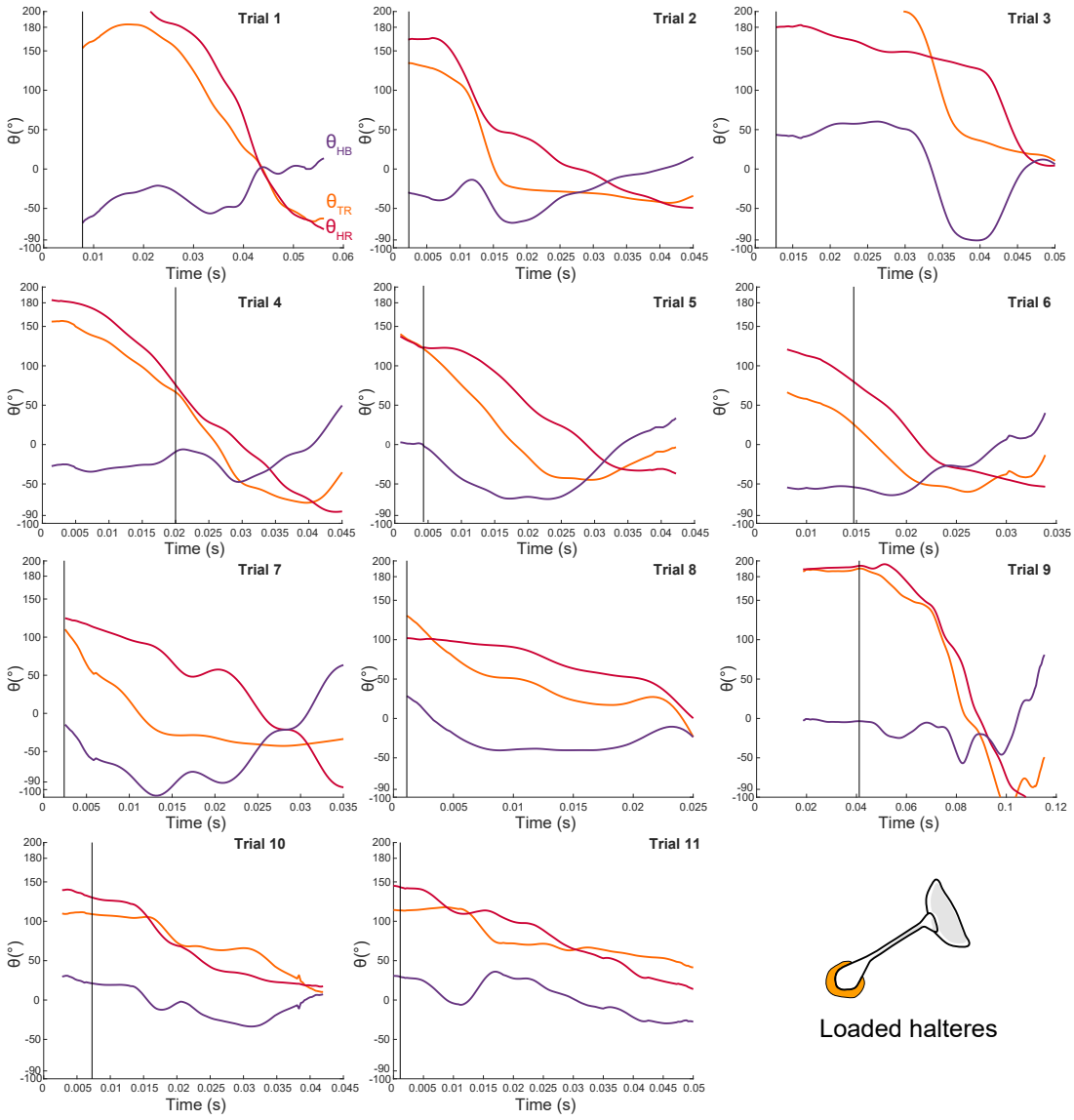

Figure 2: Plots of head, body and head/body angle (θ_{HR}, θ_{TR} and θ_{HB}) with time in the hoverfly *Episyrphus balteatus* in the loaded halteres condition. Right-side up and upside-down positions correspond to roll angles of 0° and 180°, respectively. The solid line indicates the onset of the first wingbeat.

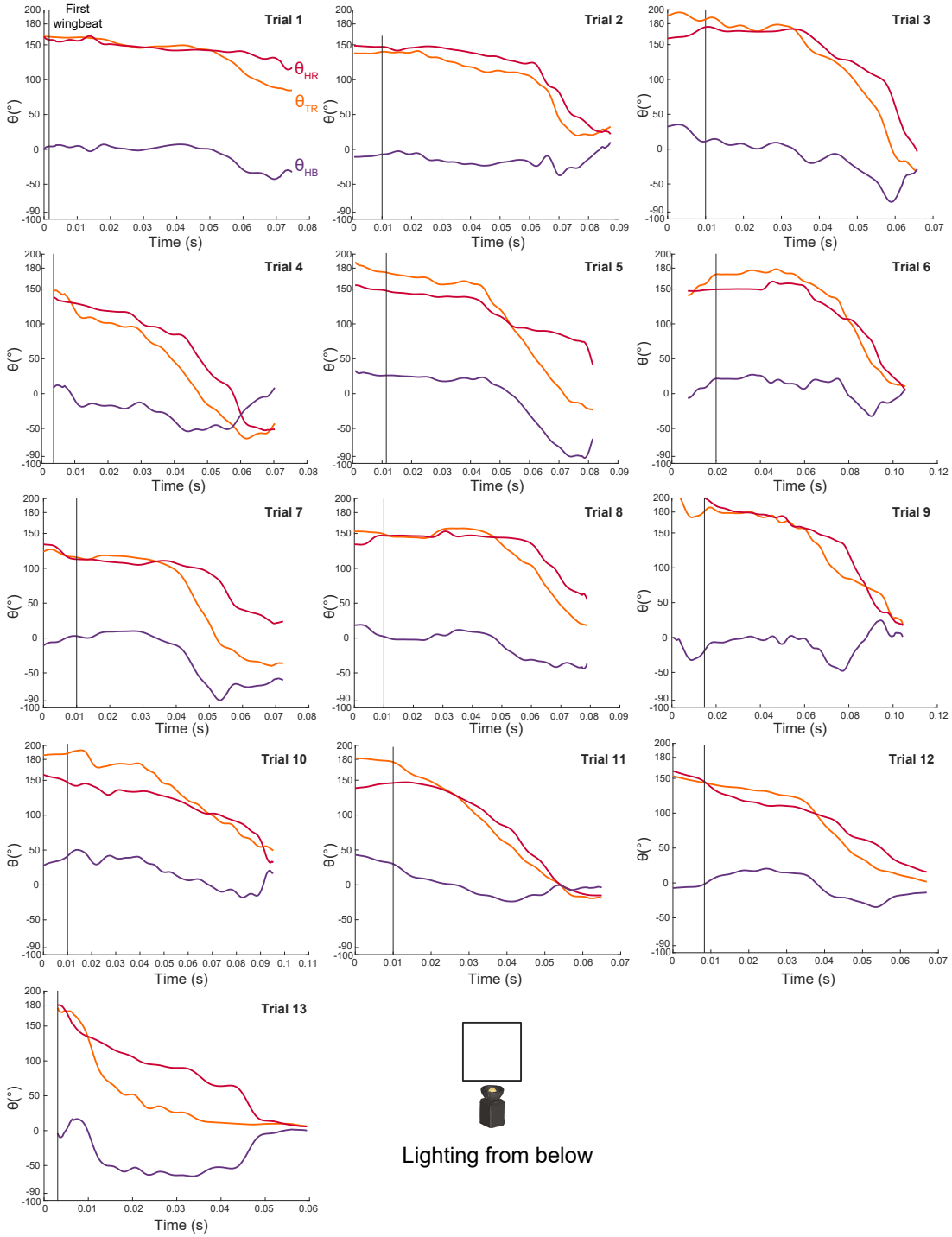

Figure 3: Plots of head, body and head/body angle (θ_{HR}, θ_{TR} and θ_{HB}) with time in the hoverfly *Episyrphus balteatus* in the lighting from below condition. Right-side up and upside-down positions correspond to roll angles of 0° and 180°, respectively. The solid line indicates the onset of the first wingbeat.

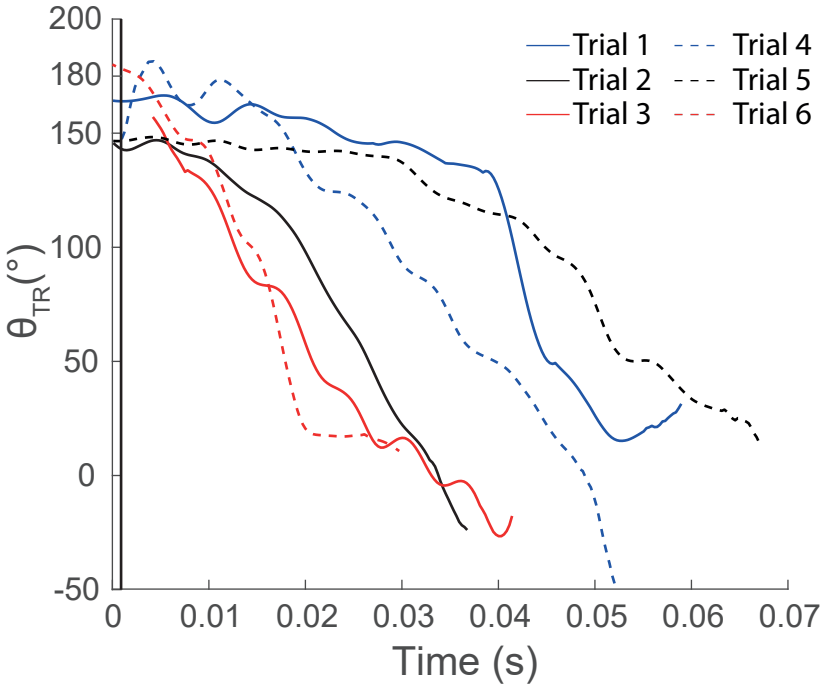

Figure 4: Plots of body angle (θ_{TR}) with time in the hoverfly Episyrphus balteatus in the head-thorax glued condition. Right-side up and upside-down positions correspond to roll angles of 0° and 180°, respectively. The vertical solid line indicates the onset of the first wingbeat.

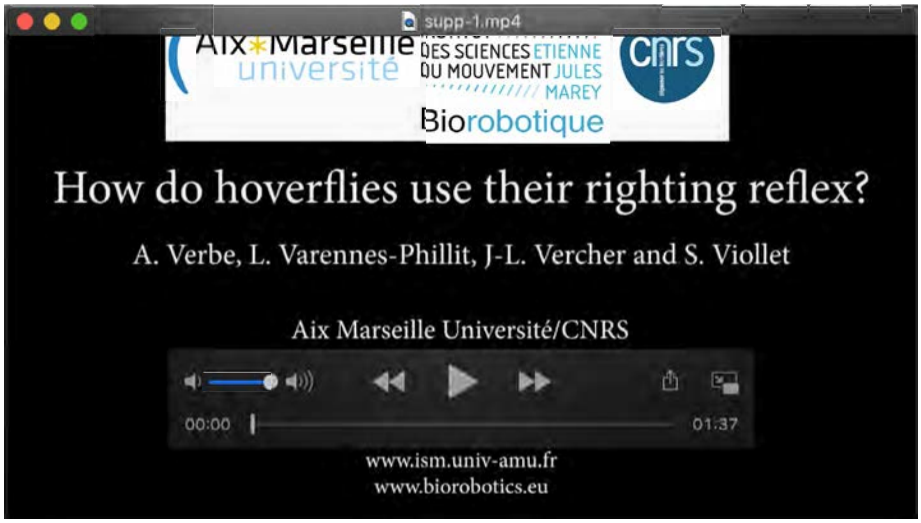

Movie 1: Video of the righting reflex in hoverflies and response of the model.